

Supplementary Information

Preparation of Bacterial Cellulose Based Nitrogen-doped Carbon Nanofibers and Their Applications in Oxygen Reduction Reaction and Sodium-ion Battery

Yang Huang ^a, Liang Wang ^c, Lei Lu ^c, Mengmeng Fan ^a, Fanshu Yuan ^a, Bianjing Sun ^a, Jieshu Qian ^{a, b, *}, Qingli Hao ^{c, *}, Dongping Sun ^{a, *}

^a Institute of Chemicobiology and Functional Materials, Nanjing University of Science and Technology, Nanjing 210094, China.

^b School of Environmental and Biological Engineering, Nanjing University of Science and Technology, Nanjing 210094, China.

^c Key Laboratory for Soft Chemistry and Functional Materials of Ministry Education, Nanjing University of Science and Technology, Nanjing 210094, China

* Corresponding authors: Prof. Jieshu Qian

E-mail: qianjieshu@foxmail.com

Tel.: +86-25-84315173

Fax: +86-25-84315352

Add.: Xiao Ling Wei 200, Nanjing, 210094, China

* Corresponding authors: Prof. Qingli Hao

E-mail: haoqingli@163.com

Tel.: +86-13851864172

Fax: +86-25-84315256

Add.: Xiao Ling Wei 200, Nanjing, 210094, China

* Corresponding authors: Prof. Dongping Sun

E-mail: sundpe301@163.com

Tel.: +86-25-84315466

Fax: +86-25-84315256

Add.: Xiao Ling Wei 200, Nanjing, 210094, China

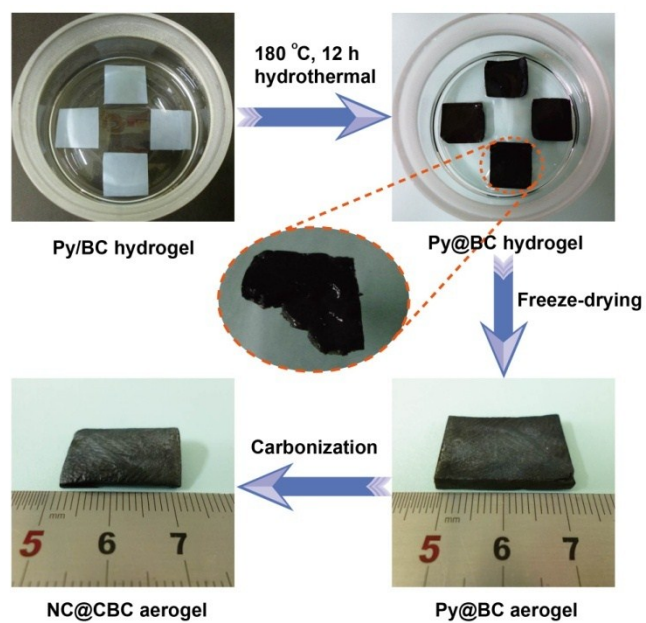


Fig. S1 Optical images showing the sample preparation involved in this work.

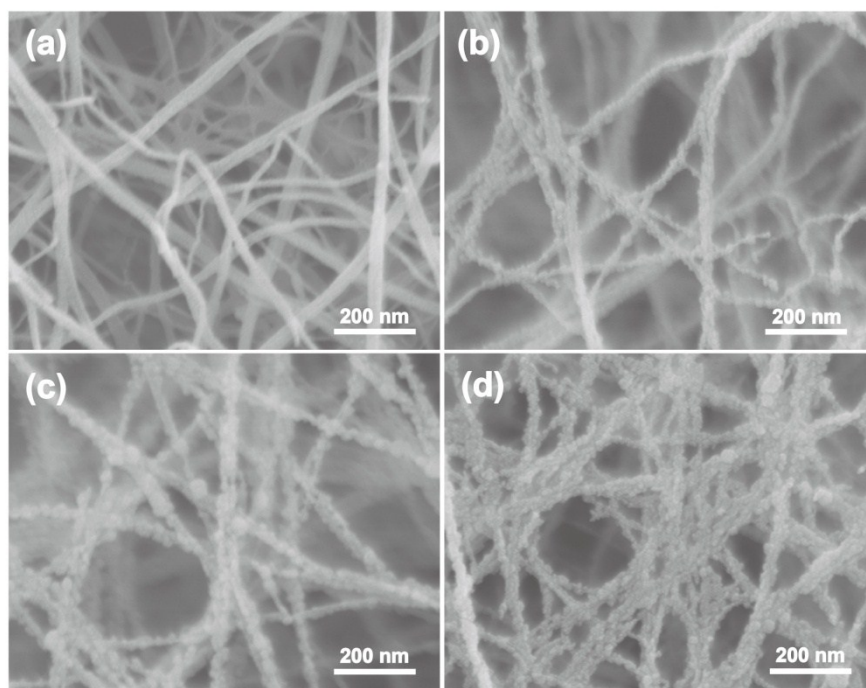


Fig. S2 Representative SEM images of (a) CBC-900, (b) NC@CBC-0.02-900, (c) NC@CBC-0.05-900, and (d) NC@CBC-0.1-900.

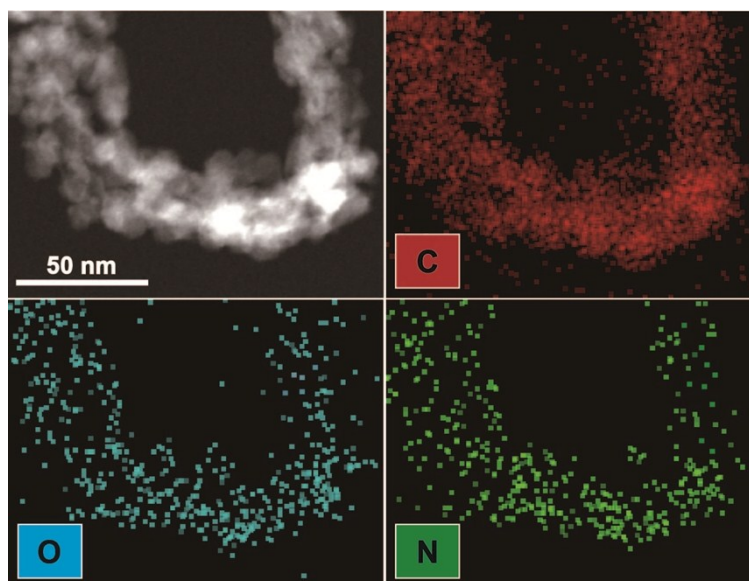


Fig. S3 STEM image of NC@CBC-0.05-900 and the corresponding elemental mapping of C (red), O (blue), and N (green).

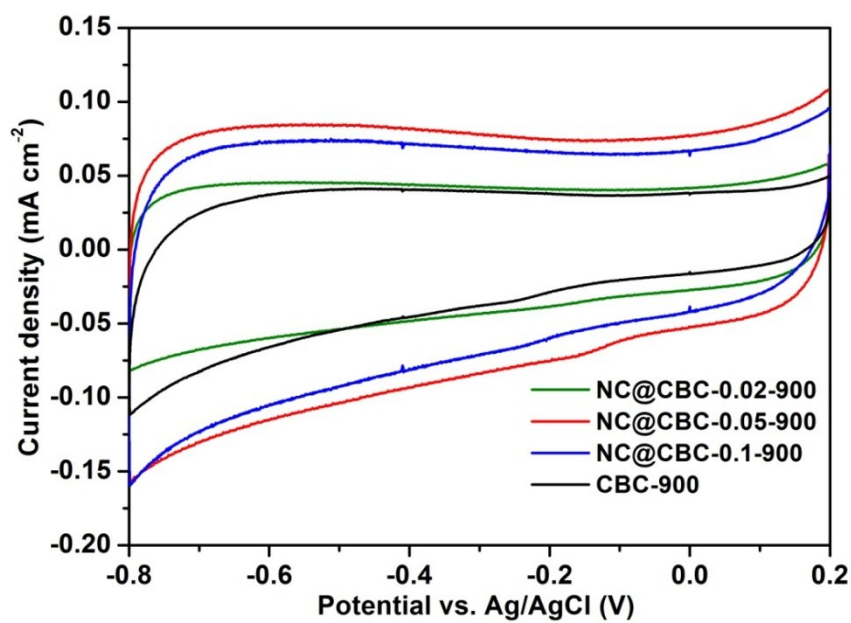


Fig. S4 CV curves of CBC-900 and NC@CBC-X-900 in N_2 -saturated 0.1 M KOH aqueous solution at a scanning rate of 10 mV s^{-1} .

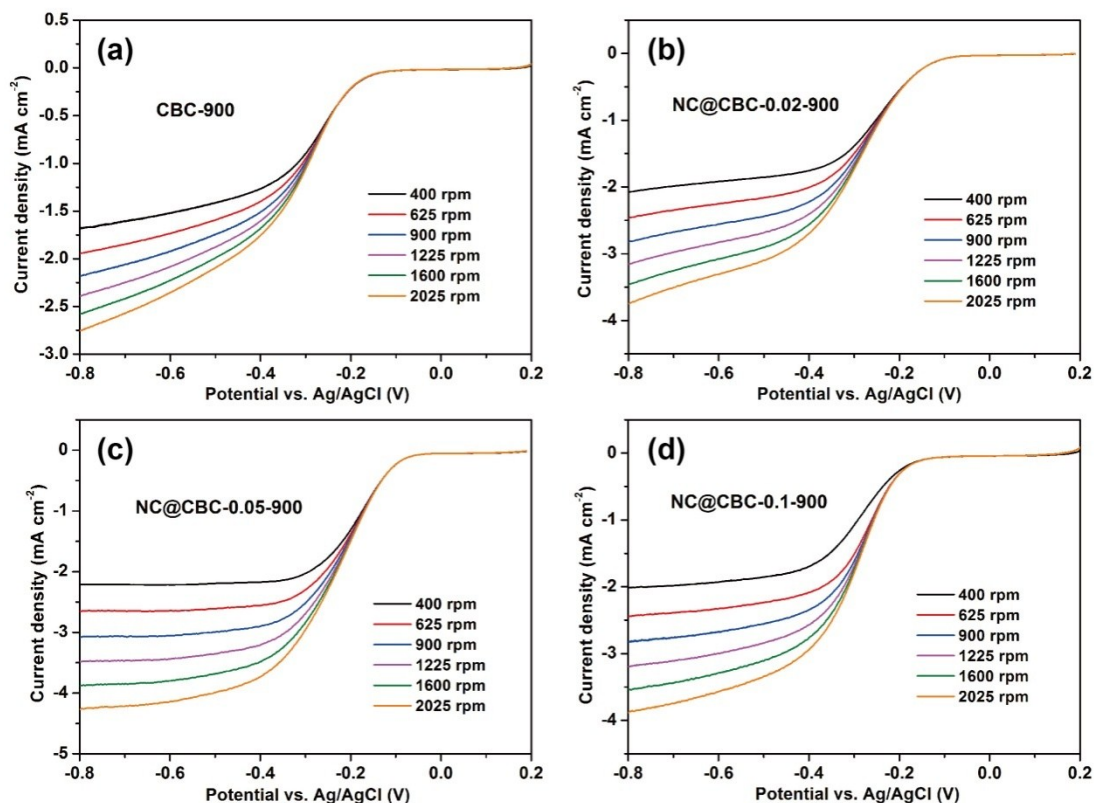


Fig. S5 LSV curves of (a) CBC-900, (b) NC@CBC-0.02-900, (c) NC@CBC-0.05-900, and (d) NC@CBC-0.1-900 in O₂-saturated 0.1 M KOH aqueous solution obtained under different rotation rates.

Table S1 Onset potential, half-wave potential, diffusion-limiting current density (J_L), and kinetic current density (J_K) of CBC-900 and NC@CBC-X-900 derived from LSV curves obtained under a consistent rotating rate of 1600 rpm.

Samples	Onset potential (V)	Half-wave potential (V) ^a	J_L (mA cm ⁻²) ^b	J_K (mA cm ⁻²) ^c
CBC-900	-0.090	-0.329	-2.576	8.78
NC@CBC-0.02-900	-0.046	-0.303	-3.462	18.21
NC@CBC-0.05-900	-0.019	-0.229	-3.877	74.71
NC@CBC-0.1-900	-0.090	-0.302	-3.541	25.60

^a Half-wave potential is calculated at which the current density is a half of the J_L

^b J_L is derived from the current density of the LSV (1600 rpm) at -0.8 V

^c J_K is calculated from the mass-transport correction of RDE with equation: $J_K = J \times J_L / (J_L - J)$

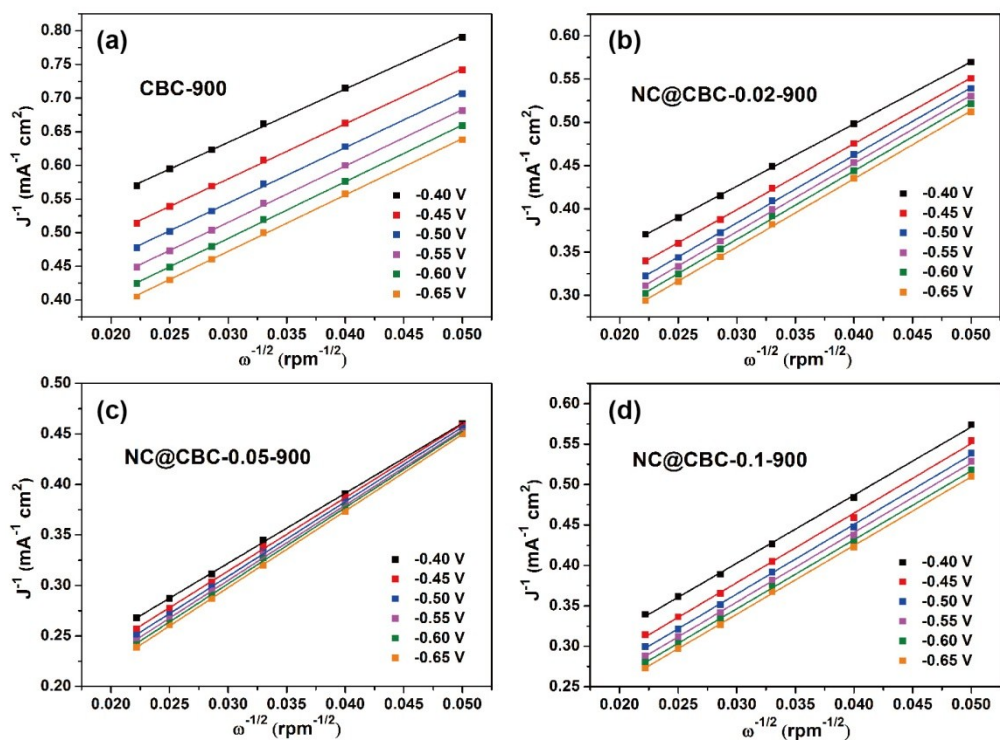


Fig. S6 K-L plots of (a) CBC-900, (b) NC@CBC-0.02-900, (c) NC@CBC-0.05-900, and (d) NC@CBC-0.1-900 at the potentials ranging from -0.65 to -0.40 V (vs. Ag/AgCl).

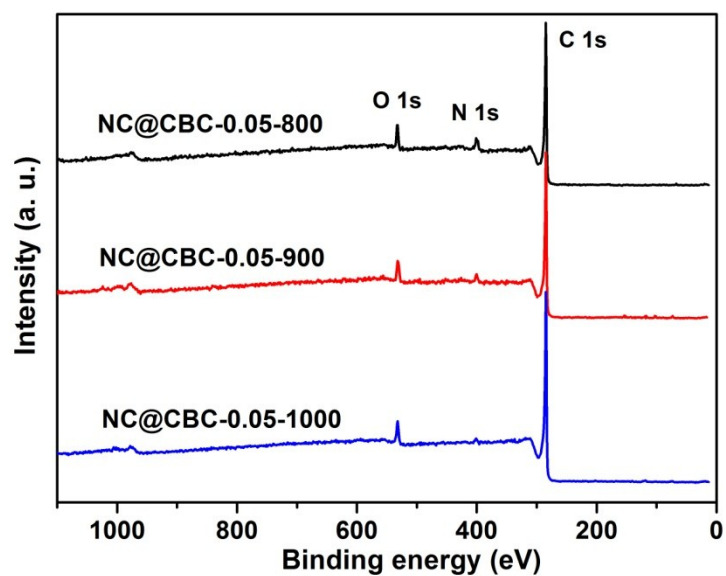


Fig. S7 XPS survey spectra of NC@CBC-0.05-800, NC@CBC-0.05-900, and NC@CBC-0.05-1000.

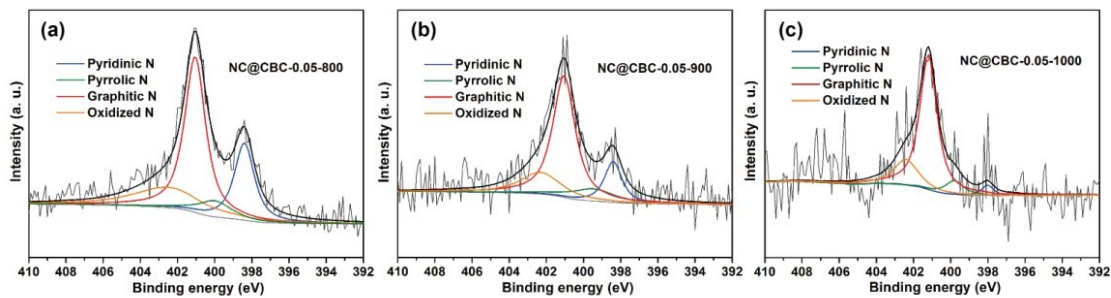


Fig. S8 XPS N1s spectra of (a) NC@CBC-0.05-800, (b) NC@CBC-0.05-900 and (c) NC@CBC-0.05-1000.

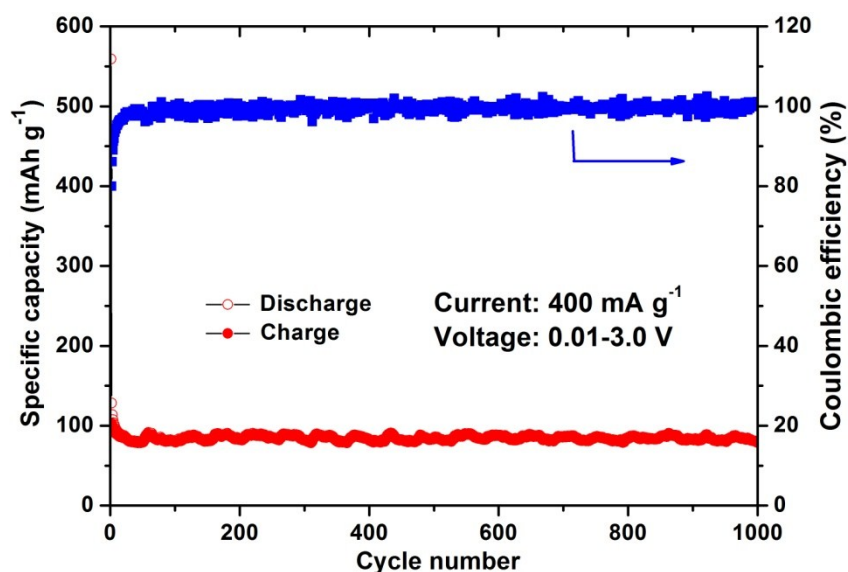


Fig. S9 Long-term cycle performance of CBC-900 as anode in SIBs at a current density of 400 mA g^{-1} .

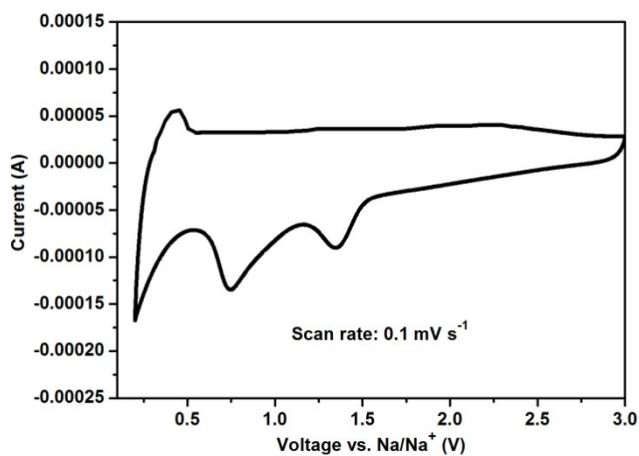


Fig. S10 The first CV cycle of NC@CBC-0.05-900 as anode in SIBs at a scan rate of 0.1 mV s^{-1} .

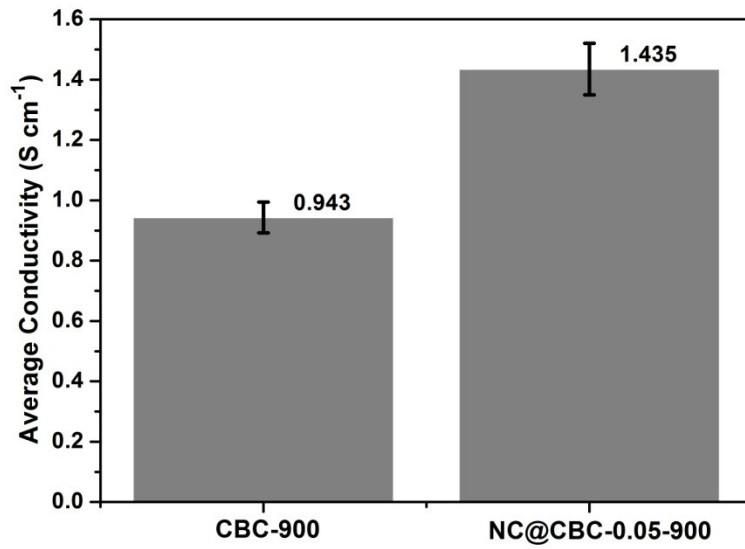


Fig. S11 Comparison of conductivity between CBC-900 and NC@CBC-0.05-900.

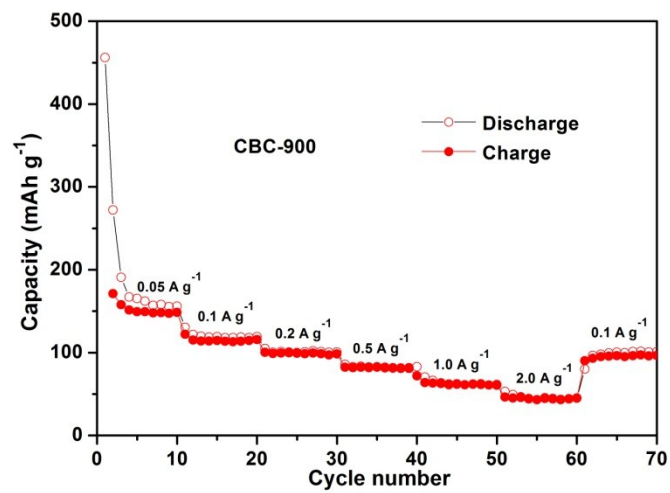


Fig. S12 Rate performance of CBC-900 electrode at various current densities.